ARTICLE

doi:10.1038/nature12143

Hypothalamic programming of systemic ageing involving IKK-β, NF-κB and GnRH

Guo Zhang[1,2,3]*, Juxue Li[1,2,3]*, Sudarshana Purkayastha[1,2,3]*, Yizhe Tang[1,2,3]*, Hai Zhang[1,2,3]*, Ye Yin[1,2,3], Bo Li[1,2,3], Gang Liu[1,2,3] & Dongsheng Cai[1,2,3]

Ageing is a result of gradual and overall functional deteriorations across the body; however, it is unknown whether an individual tissue primarily works to mediate the ageing progress and control lifespan. Here we show that the hypothalamus is important for the development of whole-body ageing in mice, and that the underlying basis involves hypothalamic immunity mediated by IκB kinase-β (IKK-β), nuclear factor κB (NF-κB) and related microglia–neuron immune crosstalk. Several interventional models were developed showing that ageing retardation and lifespan extension are achieved in mice by preventing ageing-related hypothalamic or brain IKK-β and NF-κB activation. Mechanistic studies further revealed that IKK-β and NF-κB inhibit gonadotropin-releasing hormone (GnRH) to mediate ageing-related hypothalamic GnRH decline, and GnRH treatment amends ageing-impaired neurogenesis and decelerates ageing. In conclusion, the hypothalamus has a programmatic role in ageing development via immune–neuroendocrine integration, and immune inhibition or GnRH restoration in the hypothalamus/brain represent two potential strategies for optimizing lifespan and combating ageing-related health problems.

Ageing is characterized by the gradual and overall loss of various physiological functions, leading to the end of lifespan. Although the search for resolution of ageing pathology is continuing[1–6], research has shown that certain neurons can mediate environmental influences on ageing in *Caenorhabditis elegans* and *Drosophila*, and neural manipulations of insulin or insulin-like growth factor 1 signalling or uncoupling protein 2 were shown to affect lifespan in animals[7–11]. In this study, we have focused on the hypothalamus, a key brain region that is crucial for the neuroendocrine interaction between the central nervous system and the periphery. We asked whether the hypothalamus may have a fundamental role in ageing development and lifespan control, in addition to its critical involvement in basic life-supporting functions such as growth, reproduction and metabolism. In tackling this bold question, we increasingly appreciated that an atypical collection of hypothalamic inflammatory changes can broadly and causally underlie the development of metabolic syndrome components including being overweight, glucose intolerance and hypertension[12–15], and of note, all of these disorders are often related to ageing. Furthermore, we have noted recent literature showing that microglia are involved in neurodegenerative diseases[16–24], which aligns with the appreciated connection between systemic immunity and ageing[25,26]. Here, through targeting hypothalamic immunity/inflammation, we designed to test whether the hypothalamus is fundamentally important for ageing and lifespan control.

Ageing-dependent hypothalamic NF-κB activation

In studying the potential role of the hypothalamus in ageing, we developed a strategy of targeting hypothalamic immunity, and as shown in our recent work[12–15], infection-unrelated inflammatory changes in the mediobasal hypothalamus (MBH) contribute to the development of various metabolic syndrome components, and the molecular basis is mediated crucially by NF-κB and its upstream IKK-β. Indeed, using phosphorylation of NF-κB subunit RelA to report NF-κB activation, we observed that although hypothalamic NF-κB was barely active in mice of young age (3–4 months), it was activated in the hypothalamus of mice at middle–old ages (11–13 months), and the activities further increased as the mice became older (22–24 months) (Fig. 1a, b). Agreeing with this observation, messenger RNA levels of many cytokines and immune regulators increased in the hypothalamus of old mice compared to the young group (data not shown). To visualize NF-κB activity in the MBH directly, we used an NF-κB reporter that induces green fluorescent protein (GFP) after the binding of NF-κB to its transcriptional response element in a lentiviral vector (Fig. 1c). After *in vitro* assessment of this approach (Supplementary Fig. 1a, b), we performed animal experiments by delivering this lentiviral NF-κB reporter into the MBH of mice at young, middle–old and old ages. A prolonged recovery period was used to minimize the procedure-related nonspecific effects on NF-κB. We found that GFP was negligible in the MBH of young mice (Fig. 1c), but was evident in the MBH of middle–old mice and became more profound in old mice (Fig. 1c, d), confirming that ageing is associated with hypothalamic NF-κB activation. We also injected this lentiviral NF-κB reporter into various other brain regions, and comparatively, the MBH was most sensitive to ageing-related NF-κB activation (Supplementary Fig. 1c–e). Of interest, immunostaining with the neuronal marker NeuN revealed that NF-κB activation in neurons was relatively modest under middle–old ageing, but became prominent when age further increased (Fig. 1c, d). Thus, ageing development is characterized by chronic activation of NF-κB-directed innate immune pathway predominantly in the hypothalamus.

Control of ageing by hypothalamic IKK-β and NF-κB

We then tested our proposed involvement of IKK-β and NF-κB in the hypothalamic control of ageing, and our experiments focused on the MBH. Using MBH-directed lentiviral gene delivery as we previously established[12,13], we delivered dominant-negative IκB-α (^{DN}IκB-α) to inhibit NF-κB, and constitutively active IKK-β (^{CA}IKK-β) to activate NF-κB in MBH neurons; MBH delivery of GFP in the same lentiviral

[1]Department of Molecular Pharmacology, Albert Einstein College of Medicine, Bronx, New York 10461, USA. [2]Diabetes Research Center, Albert Einstein College of Medicine, Bronx, New York 10461, USA. [3]Institute of Aging, Albert Einstein College of Medicine, Bronx, New York 10461, USA.
*These authors contributed equally to this work.

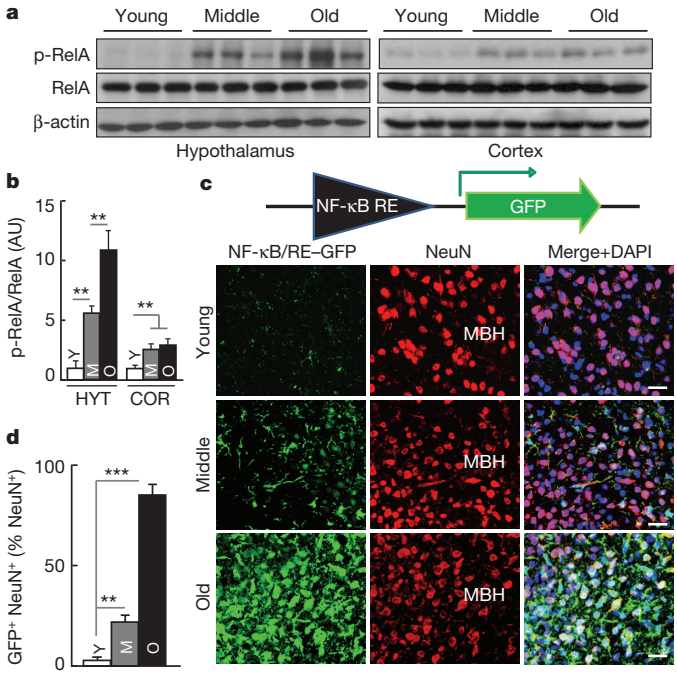

Figure 1 | Ageing-dependent hypothalamic NF-κB activation. C57BL/6 mice (chow-fed males) were analysed at young (3–4 months) age (Y), middle–old (11–13 months) age (M), and old (22–24 months) age (O). **a**, Hypothalamus and cortex were analysed via western blots. **b**, The intensity of phosphorylated RelA (p-RelA) normalized to RelA in hypothalamus (HYT) and cortex (COR). AU, arbitrary units. **c**, **d**, Mice received MBH injections of lentiviral GFP controlled by NF-κB response element (NF-κB/RE), and after a ~3-week recovery, brain sections were made to reveal GFP and NeuN stainining. 4′,6-diamidino-2-phenylindole (DAPI) staining shows entire cell populations. Scale bars, 25 μm. **c**, Images of MBH subregion. **d**, Percentages of cells co-expressing GFP and NeuN (GFP^+ $NeuN^+$) among NeuN-expressing cells ($NeuN^+$) in the MBH. $^{**}P < 0.01$; $^{***}P < 0.001$; $n = 6$ (**b**) and 3 (**d**) per group. Error bars reflect mean ± s.e.m.

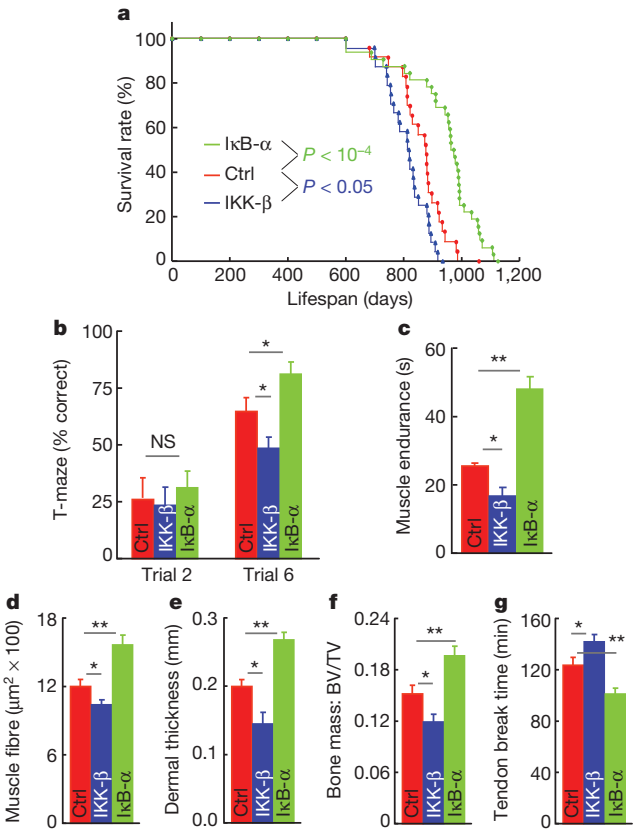

Figure 2 | Ageing manipulations by hypothalamic IKK-β and NF-κB. MBH–IKK-β, MBH–IκB-α and MBH–ctrl mice were generated using ~18-month-old C57BL/6 mice (chow-fed males) via MBH injections of lentiviruses expressing ^{CA}IKK-β, ^{DN}IκB-α and control GFP under the control of synapsin promoter. **a**, Lifespan of these mice ($n = 23$–31 mice per group). **b**, **c**, Mice at ~6 months after gene delivery were assessed for cognition via the T-maze (**b**) and muscle endurance (**c**). **d**–**g**, Mice were killed at 8–10 months after gene delivery for measuring muscle (quadriceps) fibre size (**d**), dermal thickness (**e**), bone mass (**f**), and tail tendon breaking time (**g**). BV, trabecular bone volume; TV, total tissue volume. $^{*}P < 0.05$; $^{**}P < 0.01$; MBH–ctrl: $n = 23$ (**a**), 9 (**b**), 6 (**c**), 3 (**d**, **e**), 4 (**f**) and 7 (**g**); MBH–IKK-β: $n = 24$ (**a**), 10 (**b**), 6 (**c**), 3 (**d**, **e**), 4 (**f**) and 5 (**g**); MBH–IκB-α: $n = 31$ (**a**), 12 (**b**), 7 (**c**), 3 (**d**, **e**), 6 (**f**) and 8 (**g**). Error bars reflect mean ± s.e.m.

system was used as the control (Supplementary Fig. 2a). Middle–old C57BL/6 mice received bilateral MBH lentiviral injections; use of middle–old age mice helped to eliminate developmental concerns, and, indeed, ageing retardation can be achieved through intervention starting at a middle–old age[27]. These mice with MBH delivery of ^{DN}IκB-α, ^{CA}IKK-β and control GFP were named MBH–IκB-α, MBH–IKK-β and MBH–ctrl mice, respectively, and all mice were maintained under pair feeding of a normal chow so that they had similar daily food intake. Our longitudinal follow-up revealed that MBH–ctrl mice displayed a typical pattern of lifespan (Fig. 2a), which indicated that our approach of MBH injection was technically suitable. Importantly, we found that lifespan significantly increased in MBH–IκB-α mice but decreased in MBH–IKK-β mice compared to controls (Fig. 2a). In parallel with lifespan analysis, separate mice were generated to evaluate ageing-related physiology and histology. We assessed cognition and muscle endurance of mice at ~6 months after gene delivery, at which hypothalamic NF-κB remained overactivated in MBH–IKK-β mice but suppressed in MBH–IκB-α mice (Supplementary Fig. 2b). In cognitive tests, we found that compared to controls, MBH–IκB-α mice performed better but MBH–IKK-β mice performed worse (Fig. 2b), and all of these mice were technically eligible for the test (Supplementary Fig. 2c). These mice were also subjected to a grip test, showing that ageing-related muscle weakness was attenuated in MBH–IκB-α mice but worsened in MBH–IKK-β mice (Fig. 2c). Furthermore, these mice were examined for a panel of histological biomarkers including muscle size, skin thickness, bone mass, and tail tendon collagen cross-linking. As shown in Fig. 2d–g, ageing-related changes of these biomarkers were dampened in MBH–IκB-α mice but exacerbated in MBH–IKK-β mice. Finally, given that these data were based on males, we further generated female mouse models, and results from females agreed with the observations in males (Supplementary Fig. 3). In summary, the hypothalamus has a unique role in the development of systemic ageing, and hypothalamic IKK-β and NF-κB represents a driving force in this process.

Hypothalamic microglia in ageing development

To understand ageing-related hypothalamic immunity/inflammation further, we profiled microglia in the hypothalamus. Using immunostaining, we found that numbers of microglial cells in the MBH increased in an age-dependent manner (Fig. 3a, b). Overproduction of tumour necrosis factor-α (TNF-α) (Fig. 3a, c) and activation of NF-κB (Supplementary Fig. 4) were both detected in these microglial cells, indicating that they were inflammatory. We noted that under early ageing, NF-κB activation was already evident in hypothalamic microglia (Fig. 3a, b); however, this change was still modest in hypothalamic neurons (Fig. 1c, d). Also as observed, TNF-α overproduction was mostly limited to hypothalamic microglia during early ageing, but became prevalent across the MBH, which affected other neural cells (such as neurons) in this region. We additionally measured hypothalamic *Tnfa* mRNA levels in mice of different ages, and data obtained (Supplementary Fig. 5a) well correlated with cell counting of TNF-α immunostaining (Fig. 3c). It should be mentioned that TNF-α is a gene product of NF-κB and also acts to

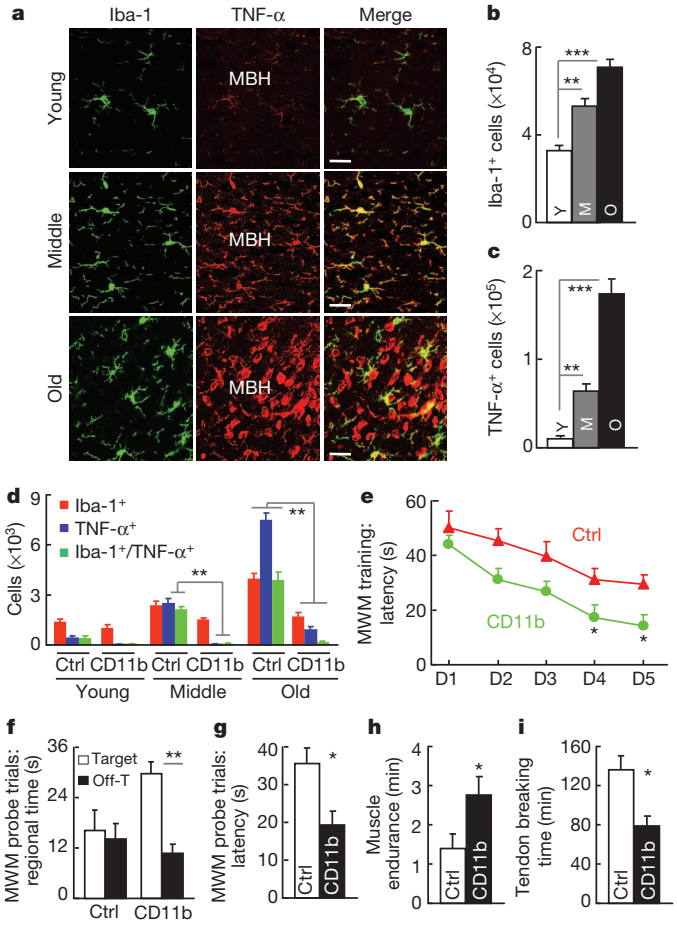

Figure 3 | Role of hypothalamic microglia in ageing. **a**–**c**, Brain sections of young, middle–old and old C57BL/6 mice were analysed for hypothalamic microglia. **a**, Images of immunostaining in MBH subregion. Scale bars, 25 μm. **b**, **c**, Numbers of cells expressing Iba-1 (Iba-1$^+$) (**b**) or TNF-α (TNF-α$^+$) (**c**) in the hypothalamic medial basal region (across the confocal microscopic field of serial sections under ×200 magnification). **d**, Middle–old *Ikbkb*$^{lox/lox}$ mice received bilateral MBH injections of lentiviral CD11b promoter-driven Cre (CD11b) versus control (ctrl). At 1 or 8 months after injection, brain sections were made for Iba-1 and TNF-α staining (images in Supplementary Fig. 4c). Mice generated at a young age provided normal references. Data show numbers of cells immunoreactive for Iba-1, TNF-α or both in the arcuate nucleus. **e**–**i**, Mice were generated via viral injections at a middle–old age and assessed at old ages for cognition (**e**–**g**), muscle endurance (**h**), and tail tendon breaking time (**i**). Morris water maze (MWM) data included time in target quadrant versus one representative off-target (off-T) quadrant in probe trials. D1–D5, days 1–5. $^*P < 0.05$; $^{**}P < 0.01$; $^{***}P < 0.001$; $n = 4$ (**b**, **c**) and 3 (**d**) per group; ctrl: $n = 6$ (**e**–**g**, **i**) and 9 (**h**); CD11b: $n = 5$ (**e**–**g**) and 6 (**h**, **i**). Error bars reflect mean ± s.e.m.

activate IKK-β and NF-κB. Overall, our data indicate that TNF-α is generated mainly by microglia during early ageing, and the paracrine actions of this cytokine on neighbouring cells is predicted to lead to ageing-associated neuronal IKK-β and NF-κB activation. In the literature, TNF-α is known to be neurotoxic or neuroprotective[28–30], which may reflect the differential functions of soluble versus transmembrane TNF-α (ref. 30). In our ageing model, soluble TNF-α seems to be involved in IKK-β and NF-κB-mediated microglia–neuron crosstalk that controls systemic ageing.

Hypothalamic control of ageing by microglial IKK-β

Subsequently, we generated a mouse model with IKK-β knockout in the MBH microglia through bilaterally delivering microglia-specific (CD11b promoter-driven) lentiviral Cre into the MBH of *Ikbkb*$^{lox/lox}$ mice, and control mice were *Ikbkb*$^{lox/lox}$ mice injected with Cre-deficient lentiviruses. Our assessment confirmed that Cre was delivered specifically in ionized calcium binding adaptor molecule 1 (Iba-1)-expressing microglia, and most of these cells in the MBH were induced with Cre (Supplementary Fig. 5b). By profiling these IKK-β knockout mice and matched controls, both of which were generated at a middle–old age, we observed that IKK-β ablation in microglia prevented against the increase of microglial cells over ageing (Fig. 3d and Supplementary Fig. 5c). Moreover, IKK-β ablation prevented ageing from inducing TNF-α expression not only in microglia but also in neighbouring cells. Such ageing-related hypothalamic microglia–neuron crosstalk via IKK-β and NF-κB led us to predict that microglia-specific IKK-β ablation might slow down ageing. To test this prediction, we continued to use this IKK-β knockout mouse model generated at a middle–old age, maintained them until old ages, and assessed their ageing manifestations. After technical evaluation (Supplementary Fig. 5d–f), we tested these mice using the Morris water maze, and data showed that microglia-specific IKK-β ablation reduced ageing-related cognitive decline (Fig. 3e–g). Furthermore, IKK-β ablation resulted in improvements in ageing-related muscle weakness (Fig. 3h) and tail collagen cross-linking (Fig. 3i). Altogether, hypothalamic microglia can act via IKK-β and NF-κB to contribute to the role of the hypothalamus in ageing development.

Genetic longevity by suppressing brain IKK-β

We further resorted to a genetic model of brain-specific IKK-β knockout mice, *N/Ikbkb*$^{lox/lox}$ mice, which we generated by breeding nestin-Cre with *Ikbkb*$^{lox/lox}$ mice as described previously[13]. Compared to wild-type littermates with matched *Ikbkb*$^{lox/lox}$ background, these knockout mice were developmentally indistinguishable in terms of brain size and gross morphology (Supplementary Fig. 6). We also compared *Ikbkb*$^{lox/lox}$ mice to additional types of control, and confirmed that all these mice were similar across a spectrum of ageing-related physiological and histological changes (Supplementary Fig. 7). In this context, we profiled ageing-related physiology and pathology in *N/Ikbkb*$^{lox/lox}$ mice and littermate wild types. At an old age, after technical assessment (Supplementary Fig. 8a–c), we subjected mice to the Morris water maze, and found that *N/Ikbkb*$^{lox/lox}$ mice outperformed wild types (Fig. 4a). This cognitive improvement was specific to ageing, because young *N/Ikbkb*$^{lox/lox}$ mice and wild types performed similarly (Supplementary Fig. 8d–h). Thus, although NF-κB seems to have a role in the development of hippocampal synaptic plasticity[31–33], the net effect from suppressing brain IKK-β and NF-κB under the ageing model is cognitively beneficial. Using a grip test, we further found that compared to wild type, *N/Ikbkb*$^{lox/lox}$ mice had a reduced extent of ageing-related muscle weakness (Fig. 4b). Also, as shown in Fig. 4c–h, *N/Ikbkb*$^{lox/lox}$ mice were protected against ageing-induced muscle and skin atrophy, bone loss and collagen cross-linking. In addition to males, female *N/Ikbkb*$^{lox/lox}$ mice were studied, and the findings were consistent (Supplementary Fig. 9). Notably, we did lifespan analysis by following a cohort of male *N/Ikbkb*$^{lox/lox}$ mice and wild-type littermates. As shown in Fig. 4i, wild-type mice had a typical pattern of median and maximal lifespan; by contrast, *N/Ikbkb*$^{lox/lox}$ mice showed a pronounced phenotype of longevity, with median lifespan 23% longer ($P = 0.0002$) and maximal lifespan 20% longer ($P < 0.05$) than wild types. We recognize that the longevity phenotype of this genetic model could be a result of IKK-β inhibition jointly in neurons and glia, as nestin-Cre is known to target neural stem/progenitor cells and derived neurons and glia. To summarize, longevity in this genetic model considerably recapitulates ageing retardation from hypothalamic IKK-β and NF-κB inhibition, and technologically, ageing retardation can be achieved via IKK-β and NF-κB inhibition across the brain without evident side effects or compromised efficacy.

Ageing-related NF-κB-induced GnRH decline

To depict the hypothalamic control of ageing better, we focused on neuroendocrine pathways of the hypothalamus, and found that IKK-β and NF-κB negatively regulated GnRH. The classical action of GnRH

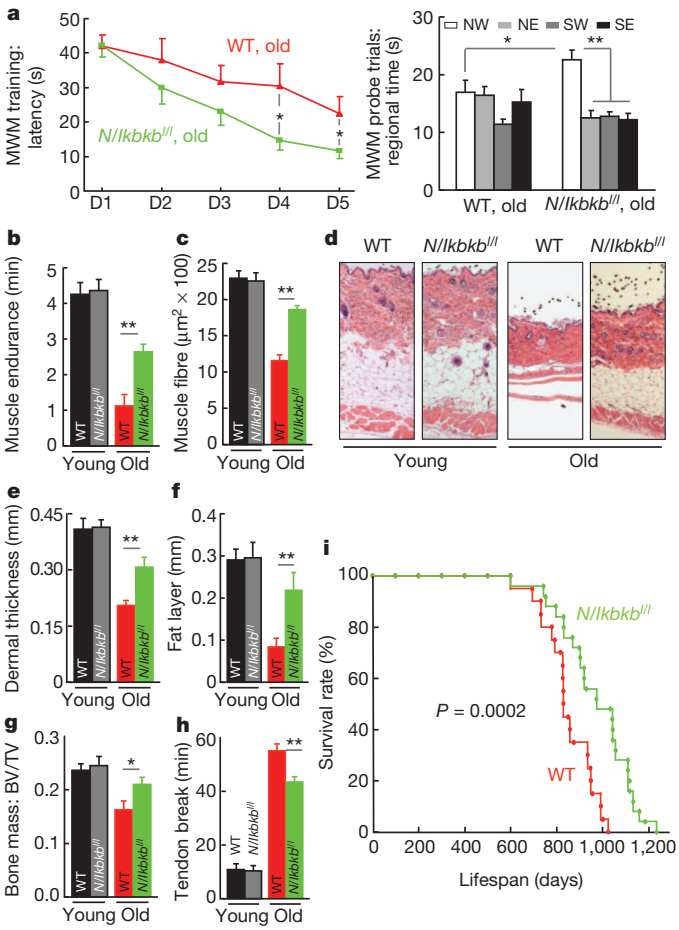

Figure 4 | Genetic longevity by brain-specific IKK-β knockout. *N/Ikbkb*$^{lox/lox}$ mice (*N/Ikbkb*$^{l/l}$) and wild-type (WT) littermates males were maintained on chow since weaning. **a**, **b**, Young (3 months) and old-age (18–20 months) mice were tested for cognition (**a**) and muscle endurance (**b**). Morris water maze data included time in target northwest (NW) versus off-target northeast (NE), southwest (SW) and southeast (SE) quadrants in probe trials. **c**–**h**, Young (3–4 months) and old (20–24 months) mice were killed for assessing muscle (quadriceps) fibre size (**c**), dermal thickness (**d**–**f**), bone mass (**g**), and tail tendon breaking time (**h**). **i**, Lifespan follow-up ($n = 20$ in wild type and $n = 25$ in *N/Ikbkb*$^{l/l}$). $^{*}P < 0.05$; $^{**}P < 0.01$; young wild type: $n = 10$ (**b**), 3 (**c**, **e**), 5 (**f**), 6 (**g**) and 8 (**h**); young *N/Ikbkb*$^{l/l}$: $n = 14$ (**b**), 3 (**c**, **e**, **f**), 6 (**g**) and 8 (**h**); old wild type: $n = 10$ (**a**), 7 (**b**), 3 (**c**, **e**), 5 (**f**, **g**) and 6 (**h**); old *N/Ikbkb*$^{l/l}$: $n = 10$ (**a**), 7 (**b**), 3 (**c**, **e**, **f**) and 6 (**g**, **h**). Error bars reflect mean ± s.e.m.

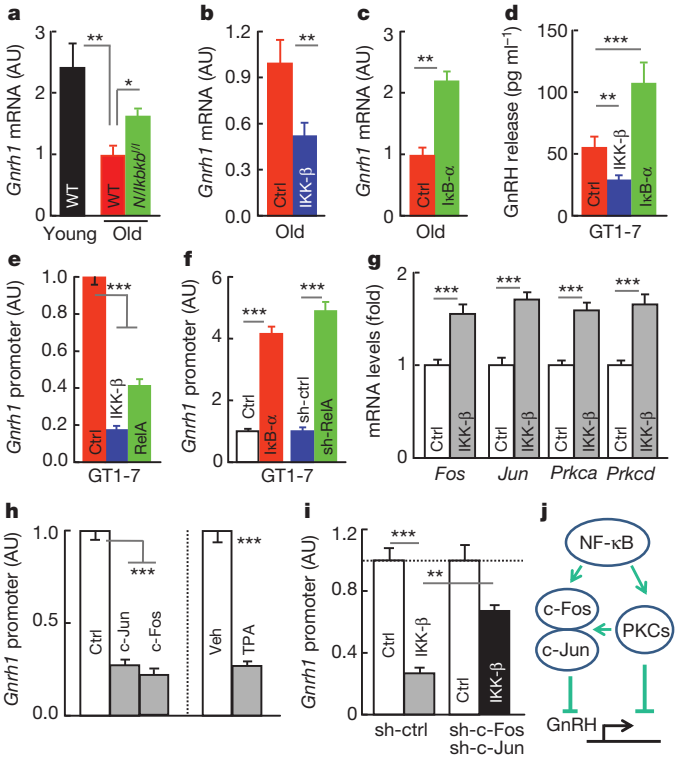

Figure 5 | Inhibition of GnRH by IKK-β and NF-κB. **a**–**c**, Hypothalamic *Gnrh1* mRNA of mice described in Figs 2 and 3. **d**–**g**, GT1-7 cells were transfected with ^{CA}IKKβ, RelA or ^{DN}IκBα or control plasmid (**d**, **e**, **g**), co-transfected with *Gnrh1*-promoter luciferase plasmid (**e**, **f**), or together with *Rela* short hairpin RNA (shRNA) (sh-RelA) or control shRNA (sh-ctrl) plasmid (**f**), and were measured for GnRH release (**d**), *Gnrh1* promoter (**e**, **f**), and *Fos*, *Jun*, *Prkca* and *Prkcd* mRNA levels (**g**). **h**, *Gnrh1* promoter activities were measured for GT1-7 cells transfected with *Gnrh1*-promoter luciferase plasmid, co-transfected with c-Jun or c-Fos plasmid versus control plasmid, or treated with 12-*O*-tetradecanoylphorbol-13-acetate (TPA) or vehicle (veh). **i**, *Gnrh1* promoter activities were measured for GT1-7 cells transfected with *Gnrh1*-promoter luciferase plasmid, co-transfected with ^{CA}IKKβ or control plasmid, and with *Fos* and *Jun* shRNA plasmids (sh-c-Fos and sh-c-Jun) or scramble shRNA control (sh-ctrl). Values in both control groups were normalized as 1. **j**, Summarized schematic model. $^{*}P < 0.05$, $^{**}P < 0.01$; $^{***}P < 0.001$; $n = 12$ (**a**, **e**) and 3 (**f**–**i**) per group, and $n = 6$ (**b**), 8 (**c**) and 4 (**d**) in control, $n = 8$ (**b**) and 6 (**d**) in IKK-β, and $n = 8$ (**c**) and 6 (**d**) in IκB-α. Error bars reflect mean ± s.e.m.

is to regulate sex hormones and reproduction, but whether GnRH is important for whole-body ageing has yet to be determined. We found that ageing was associated with reduced hypothalamic *Gnrh1* mRNA, and this change was reversed by IKK-β and NF-κB inhibition but enhanced by their activation (Fig. 5a–c and Supplementary Fig. 10a). Using GT1-7 cells, a cell line of GnRH neurons, we confirmed that GnRH release from these cells decreased after IKK-β and NF-κB activation, but increased after IKK-β and NF-κB inhibition (Fig. 5d). To study whether NF-κB might inhibit the *Gnrh1* gene, we introduced *Gnrh1* promoter-driven luciferase into GT1-7 cells, and simultaneously activated or inhibited IKK-β and NF-κB in these cells. Results showed that *Gnrh1* promoter activity reduced ~50% after IKK-β and NF-κB activation, but increased 4–5-fold by IKK-β and NF-κB inhibition (Fig. 5e, f). Moreover, IKK-β and NF-κB activation increased *Fos* (also known as *c-fos*), *Jun* (*c-jun*), *Prkca* (*Pkca*) and *Prkcd* (*PKCδ*) mRNA levels (Fig. 5g), and this finding was relevant because c-Fos and c-Jun overexpression and protein kinase C (PKC) activation were both able to inhibit the *Gnrh1* promoter (Fig. 5h). Furthermore, IKK-β and NF-κB inhibition of the *Gnrh1* promoter was attenuated by blocking c-Fos and c-Jun (Fig. 5i) or by suppressing the PKC pathway (Supplementary Fig. 10b). Altogether, the c-Fos, c-Jun and PKC pathways can work together to mediate the inhibitory effect of IKK-β and NF-κB on GnRH (Fig. 5j), and in conjunction with relevant literature[34], transcriptional integration of NF-κB and c-Jun seems to account for down-regulation of GnRH in the hypothalamus.

GnRH treatment prevents ageing-impaired neurogenesis

On the basis of the known role of GnRH in regulating sex hormones, GnRH changes in our mouse models might correlate with changes in sex hormones, and this prediction was proved (Supplementary Fig. 10c, d). However, a sex hormone may not be a primary mediator for ageing phenotypes in our models, because hypothalamic IKK-β and NF-κB are important for ageing in both sexes. This context provoked us to propose that GnRH works as a primary mediator independently of a specific sex hormone. To explore whether GnRH exerts intra-brain actions to affect ageing, we delivered GnRH into the hypothalamic third-ventricle of old mice, and examined ageing-related changes in brain cell biology. A notable observation was that GnRH promoted adult neurogenesis despite ageing. Using BrdU tracking following a

single BrdU injection to report neurogenesis[12], we found that ageing is characterized by diminished neurogenesis, particularly in the hypothalamus and the hippocampus; however, this defect was substantially reversed by GnRH treatment (Fig. 6a–c). Thirty-day BrdU tracking (with seven days of daily BrdU injections) also confirmed that BrdU-labelled cells in GnRH-treated mice significantly survived (Fig. 6d, e). Of note, these effects were seen in not only the hypothalamus but also the hippocampus and other brain regions (data not shown), reflecting the fact that GnRH travels within the brain to promote neurogenesis. Therefore, given the leadership role of the brain in controlling whole-body physiology, the brain-wide neurogenesis induced by hypothalamic GnRH may provide an explanation about how the hypothalamus, a very small structure in the brain, could control systemic ageing.

GnRH therapy decelerates ageing development

Finally, to study whether GnRH could affect ageing, we subjected old MBH–IKK-β mice and MBH-ctrl mice described in Fig. 2 to daily GnRH therapy for a prolonged period, and then examined their ageing physiology and histology. As we were also interested in testing whether GnRH could act peripherally to affect ageing, we treated mice with GnRH via peripheral injections. Notably, GnRH treatment reduced the magnitude of ageing histology in control mice and abrogated the pro-ageing phenotype in MBH–IKK-β mice (Fig. 6f–h). Interestingly, despite the peripheral administration, GnRH led to an amelioration of ageing-related cognitive decline (Fig. 6i and Supplementary Fig. 11). Thus, a prolonged increase of systemic GnRH can cumulatively yield actions on the brain; despite the mechanism remains to be studied, some GnRH-responsive brain regions outside of the blood–brain barrier, such as the median eminence, subfornical organ and area postrema, can have access to peripheral-delivered GnRH. These effects of GnRH were not specific to a sex, as similar outcomes were shown in males (Fig. 6f–i, Supplementary Fig. 11) and females (Supplementary Fig. 12). For comparison, we treated MBH–IκB-α mice with GnRH, and it turned out that GnRH did not further enhance the anti-ageing phenotype in MBH–IκB-α mice (Supplementary Fig. 13), suggesting that NF-κB inhibition and GnRH action may work in the same pathway to counteract ageing. Clearly, future studies are still needed to detail the central and peripheral roles of GnRH in hypothalamic control of ageing; regardless, this body of data can lead to the conclusion that the hypothalamus can integrate NF-κB-directed immunity and GnRH-driven neuroendocrine system to program ageing development.

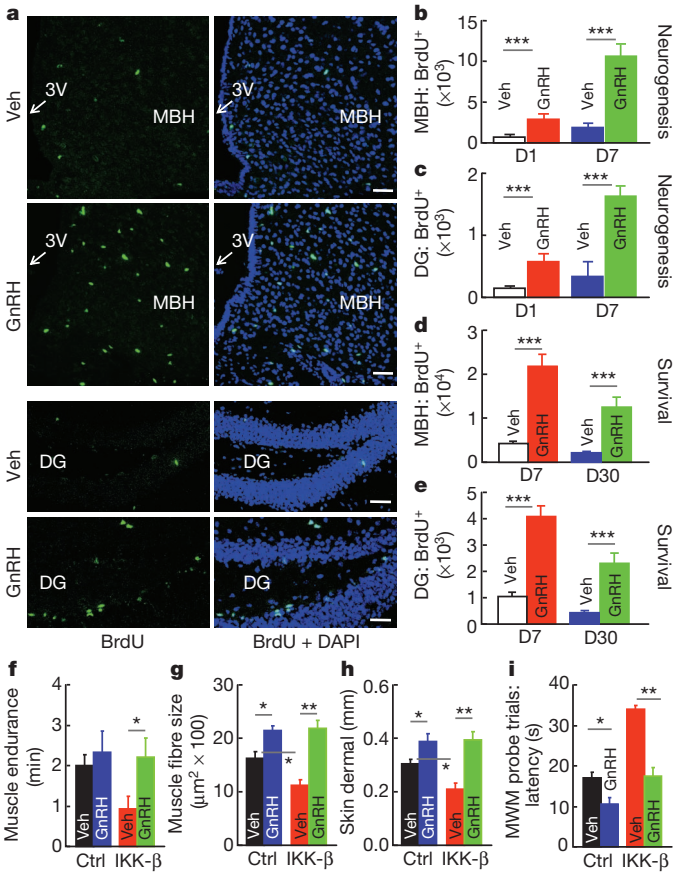

Figure 6 | Central and systemic actions of GnRH in counteracting ageing. **a**–**e**, C57BL/6 mice at an old age were subjected to neurogenesis (**a**–**c**) and survival (**d**, **e**) assays, as detailed in the Methods. **a**, BrdU staining images of MBH subregion and dentate gyrus (DG) in neurogenesis assay. 3V, third ventricle. Scale bars, 50 μm. **b**, **c**, BrdU-labelled ($BrdU^+$) cells in the MBH (**b**) and dentate gyrus (**c**) in a neurogenesis assay. **d**, **e**, Survival of BrdU-labelled ($BrdU^+$) cells in the MBH (**d**) and dentate gyrus (**e**) in a survival assay. **f**–**i**, MBH–IKK-β and MBH–ctrl mice at an old age were daily injected subcutaneously with GnRH or vehicle for 5 weeks, and analysed for muscle endurance (**f**), skeletal muscle fibres (**g**), dermal thickness (**h**) and cognition (**i**) (see Supplementary Fig. 10 for additional data). $*P < 0.05$; $**P < 0.01$; $***P < 0.001$; $n = 4$ (**b**–**e**), 7 (**f**) and 3 (**g**, **h**) per group, and $n = 12$ (control, vehicle), 7 (control, GnRH), 7 (IKK-β, vehicle) and 8 (IKK-β, GnRH) (**i**). Error bars reflect mean ± s.e.m.

Discussion

In this work, we conceived that the hypothalamus, which is known to have fundamental roles in growth, development, reproduction and metabolism, is also responsible for systemic ageing and thus lifespan control. Notably, through activating or inhibiting immune pathway IKK-β and NF-κB in the hypothalamus of mice, we were able to accelerate or decelerate the ageing process, leading to shortened or increased lifespan. Thus, in line with the literature that appreciated the effects of the nervous system on lifespan[7–11], our findings provide a proof of principle to the hypothesis that ageing is a life event that is programmed by the hypothalamus. Indeed, brain change is an early ageing manifestation[4], and we reasoned that some hypothalamic alterations may act to motivate ageing of the rest parts in the body, and this outreaching role of the hypothalamus aligns with the fact that it is the neuroendocrine 'headquarters' in the body. Along this line, we further revealed a direct link between IKK-β and NF-κB activation and GnRH decline, and also importantly, we discovered that GnRH induces adult neurogenesis broadly in the brain, and GnRH therapy can greatly amend ageing disorders. Thus, whereas the inhibition of GnRH by NF-κB may lead to the end of reproductive length—which seems necessary for species' quality—it initiates systemic ageing at the same time. Questions remain about how hypothalamic IKK-β and NF-κB is activated in this process; speculatively, as deduced from some recent studies about sirtuins and NF-κB[35,36], age increase-induced epigenetic changes might be accountable, which calls for future investigations.

To summarize, our study using several mouse models demonstrates that the hypothalamus is important for systemic ageing and lifespan control. This hypothalamic role is significantly mediated by IKK-β- and NF-κB-directed hypothalamic innate immunity involving microglia–neuron crosstalk. The underlying basis includes integration between immunity and neuroendocrine of the hypothalamus, and immune inhibition and GnRH restoration in the hypothalamus or the brain represent two potential strategies for combating ageing-related health problems.

METHODS SUMMARY

All mice in this study were in C57BL/6 background, and *Ikbkb*$^{lox/lox}$ and nestin-Cre mice were described previously[13]. Physiological analyses included open field, visual platform test, Morris water maze, T-maze and grip test. Skin and muscle histology, bone mass via X-ray microtomography, and tail tendon breaking time were examined using standard methods in the literature. Lentiviral DNAs, virus production, MBH injection, immunostaining, western blot, and real-time PCR were similarly used in our recent research[13], and described in the Methods. The *Gnrh1* promoter was analysed in GT1-7 cells transfected with *Gnrh1* promoter-driven luciferase plasmids. Lifespan analyses were performed as detailed in

Methods. Statistics included analysis of variance (ANOVA) and appropriate post-hoc analyses for comparisons involving more than two groups and two-tailed Student's *t*-test for comparisons involving only two groups. Data were presented as mean ± s.e.m. $P < 0.05$ was considered significant.

Full Methods and any associated references are available in the online version of the paper.

Received 5 October 2011; accepted 2 April 2013.
Published online 1 May 2013.

1. Miller, R. A. Genes against aging. *J. Gerontol. A Biol. Sci. Med. Sci.* **67A,** 495–502 (2012).
2. Mattson, M. P. Pathways towards and away from Alzheimer's disease. *Nature* **430,** 631–639 (2004).
3. Masoro, E. J. Overview of caloric restriction and ageing. *Mech. Ageing Dev.* **126,** 913–922 (2005).
4. Finch, C. E. Neurons, glia, and plasticity in normal brain aging. *Adv. Gerontol.* **10,** 35–39 (2002).
5. Zitnik, G. & Martin, G. M. Age-related decline in neurogenesis: old cells or old environment? *J. Neurosci. Res.* **70,** 258–263 (2002).
6. Martin, G. M. Epigenetic gambling and epigenetic drift as an antagonistic pleiotropic mechanism of aging. *Aging Cell* **8,** 761–764 (2009).
7. Bishop, N. A. & Guarente, L. Two neurons mediate diet-restriction-induced longevity in *C. elegans*. *Nature* **447,** 545–549 (2007).
8. Fridell, Y. W., Sanchez-Blanco, A., Silvia, B. A. & Helfand, S. L. Targeted expression of the human uncoupling protein 2 (hUCP2) to adult neurons extends life span in the fly. *Cell Metab.* **1,** 145–152 (2005).
9. Alcedo, J. & Kenyon, C. Regulation of *C. elegans* longevity by specific gustatory and olfactory neurons. *Neuron* **41,** 45–55 (2004).
10. Wolkow, C. A., Kimura, K. D., Lee, M. S. & Ruvkun, G. Regulation of *C. elegans* life-span by insulinlike signaling in the nervous system. *Science* **290,** 147–150 (2000).
11. Taguchi, A., Wartschow, L. M. & White, M. F. Brain IRS2 signaling coordinates life span and nutrient homeostasis. *Science* **317,** 369–372 (2007).
12. Li, J., Tang, Y. & Cai, D. IKKβ/NF-κB disrupts adult hypothalamic neural stem cells to mediate a neurodegenerative mechanism of dietary obesity and pre-diabetes. *Nature Cell Biol.* **14,** 999–1012 (2012).
13. Zhang, X. *et al.* Hypothalamic IKKβ/NF-κB and ER stress link overnutrition to energy imbalance and obesity. *Cell* **135,** 61–73 (2008).
14. Purkayastha, S. *et al.* Neural dysregulation of peripheral insulin action and blood pressure by brain endoplasmic reticulum stress. *Proc. Natl Acad. Sci. USA* **108,** 2939–2944 (2011).
15. Purkayastha, S., Zhang, G. & Cai, D. Uncoupling the mechanisms of obesity and hypertension by targeting hypothalamic IKK-β and NF-κB. *Nature Med.* **17,** 883–887 (2011).
16. Okun, E., Griffioen, K. J. & Mattson, M. P. Toll-like receptor signaling in neural plasticity and disease. *Trends Neurosci.* **34,** 269–281 (2011).
17. Glass, C. K., Saijo, K., Winner, B., Marchetto, M. C. & Gage, F. H. Mechanisms underlying inflammation in neurodegeneration. *Cell* **140,** 918–934 (2010).
18. Saijo, K. *et al.* A Nurr1/CoREST pathway in microglia and astrocytes protects dopaminergic neurons from inflammation-induced death. *Cell* **137,** 47–59 (2009).
19. Saijo, K., Collier, J. G., Li, A. C., Katzenellenbogen, J. A. & Glass, C. K. An ADIOL-ERβ-CtBP transrepression pathway negatively regulates microglia-mediated inflammation. *Cell* **145,** 584–595 (2011).
20. Saijo, K. & Glass, C. K. Microglial cell origin and phenotypes in health and disease. *Nature Rev. Immunol.* **11,** 775–787 (2011).
21. Lucin, K. M. & Wyss-Coray, T. Immune activation in brain aging and neurodegeneration: too much or too little? *Neuron* **64,** 110–122 (2009).
22. Villeda, S. & Wyss-Coray, T. Microglia–a wrench in the running wheel? *Neuron* **59,** 527–529 (2008).
23. Villeda, S. A. *et al.* The ageing systemic milieu negatively regulates neurogenesis and cognitive function. *Nature* **477,** 90–94 (2011).
24. Yoshiyama, Y. *et al.* Synapse loss and microglial activation precede tangles in a P301S tauopathy mouse model. *Neuron* **53,** 337–351 (2007).
25. Adler, A. S. *et al.* Motif module map reveals enforcement of aging by continual NF-κB activity. *Genes Dev.* **21,** 3244–3257 (2007).
26. Peng, B. *et al.* Defective feedback regulation of NF-κB underlies Sjogren's syndrome in mice with mutated κB enhancers of the IκBα promoter. *Proc. Natl Acad. Sci. USA* **107,** 15193–15198 (2010).
27. Harrison, D. E. *et al.* Rapamycin fed late in life extends lifespan in genetically heterogeneous mice. *Nature* **460,** 392–395 (2009).
28. Barger, S. W. *et al.* Tumor necrosis factors α and β protect neurons against amyloid β-peptide toxicity: evidence for involvement of a κ B-binding factor and attenuation of peroxide and Ca^{2+} accumulation. *Proc. Natl Acad. Sci. USA* **92,** 9328–9332 (1995).
29. Bruce, A. J. *et al.* Altered neuronal and microglial responses to excitotoxic and ischemic brain injury in mice lacking TNF receptors. *Nature Med.* **2,** 788–794 (1996).
30. Taoufik, E. *et al.* Transmembrane tumour necrosis factor is neuroprotective and regulates experimental autoimmune encephalomyelitis via neuronal nuclear factor-κB. *Brain* **134,** 2722–2735 (2011).
31. Kaltschmidt, B. *et al.* NF-κB regulates spatial memory formation and synaptic plasticity through protein kinase A/CREB signaling. *Mol. Cell. Biol.* **26,** 2936–2946 (2006).
32. Meffert, M. K., Chang, J. M., Wiltgen, B. J., Fanselow, M. S. & Baltimore, D. NF-κB functions in synaptic signaling and behavior. *Nature Neurosci.* **6,** 1072–1078 (2003).
33. O'Mahony, A. *et al.* NF-κB/Rel regulates inhibitory and excitatory neuronal function and synaptic plasticity. *Mol. Cell. Biol.* **26,** 7283–7298 (2006).
34. Huang, W., Ghisletti, S., Perissi, V., Rosenfeld, M. G. & Glass, C. K. Transcriptional integration of TLR2 and TLR4 signaling at the NCoR derepression checkpoint. *Mol. Cell* **35,** 48–57 (2009).
35. Kawahara, T. L. *et al.* SIRT6 links histone H3 lysine 9 deacetylation to NF-κB-dependent gene expression and organismal life span. *Cell* **136,** 62–74 (2009).
36. Michishita, E. *et al.* SIRT6 is a histone H3 lysine 9 deacetylase that modulates telomeric chromatin. *Nature* **452,** 492–496 (2008).

Supplementary Information is available in the online version of the paper.

Acknowledgements We thank other Cai laboratory members for technical assistance, and L. Farhana, D. Stocco, L. Eckhardt, T. Ohshima, A. Lin and D. Tantin for reagents. This study was supported by National Institutes of Health (NIH) grants R01 AG 031774, R01 DK078750, and American Diabetes Association grant 1-12-BS-20 (all to D.C.). D.C. is a recipient of Irma T. Hirschl Scholarship.

Author Contributions D.C. conceived project and designed the study; G.Z., J.L., S.P., Y.T., H.Z. and Y.Y. performed experiments with assistance from B.L. and G.L. All authors carried out data analyses and interpretations; D.C. organized experimentation and wrote the paper.

Author Information Reprints and permissions information is available at www.nature.com/reprints. The authors declare no competing financial interests. Readers are welcome to comment on the online version of the paper. Correspondence and requests for materials should be addressed to D.C. (dongsheng.cai@einstein.yu.edu).

METHODS

Mouse models and treatments. Nestin-Cre mice and *Ikbkb*$^{lox/lox}$ mice were described in our previous publications[13–15,37], and maintained on C57BL/6 strain for more than 15 generations. C57BL/6 mice were obtained from Jackson Laboratory or the National Institute of Ageing, NIH. All mice were kept under standard and infection-free housing, with 12-h light/12-h dark cycles and 4–5 mice per cage. Pathogen-free quality was ensured with quarterly serology, quarterly histopathological examinations and routine veterinarian monitoring, and a bacteriological test was additionally included. All mice in this study were maintained on a normal chow from LabDiet (4.07 kcal g^{-1}).

For animal GnRH therapy, mice were subcutaneously injected with GnRH (Sigma) at the dose of 2 ng per mouse on a daily basis for a period of 5–8 weeks. The Institutional Animal Care and Use Committee at the Albert Einstein College of Medicine approved all the procedures. Body weight and food intake were measured regularly using a laboratory scale. We performed the grip test to measure muscle endurance using the method as similarly described in the literature[38,39], using a homemade square grid with a small mesh size to allow mice to hang for longer time. In brief, a mouse was lifted by the tail and placed on a homemade square grid (1-cm mesh size). The grid was then inverted 30.5 cm over a soft pad, and the mouse was allowed to hang by paws for a maximum of 5 min. The time that the mouse was able to hang was recorded during a 5-min test period.

Lentiviruses and MBH injection. Synapsin promoter-directed lentiviral vector was used to drive neuron-specific gene delivery as previously established[13–15,37]. These lentiviral vectors contain the cDNA of ^{CA}IKK-β or ^{DN}IκB-α or only GFP under the control of synapsin promoter. To create lentiviral NF-κB reporter vector, a target plasmid was constructed to have the GFP open reading frame controlled by a DNA cassette containing five tandem repeats of the NF-κB transcriptional response element, according to the approach established in the literature[40]. The lentiviruses were produced from HEK293T cells via co-transfecting a target plasmid with two package plasmids (VSVg and delta 8.9) using $CaCl_2$. Lentiviruses were purified through ultracentrifugation. Intra-MBH viral injections were performed as we previously established[13–15,37]. In brief, under an ultraprecise stereotactic instrument (resolution: 10 μm) (Kopf Instruments), lentiviruses were bilaterally injected at the coordinates of 1.5 mm posterior to the bregma, 5.8 mm below the skull, and 0.2 mm lateral to the midline.

Cognitive behavioural tests. All mice were tested for general health, sensorimotor reflexes and motor responses before the onset of all behavioural testing. Mice were maintained on a 12-h light/12-h dark schedule in an isolation unit located inside the behavioural testing room. An Anymaze video tracking system (Stoelting) equipped with a digital camera connected to a computer was used to videotape the whole course of animal activities in training and experimental sessions of behavioural tests.

Open field test. Locomotor activities were assessed using the open field test. The open field arena consisted of a clear Plexiglas chamber that was 40 cm × 40 cm, with walls that were 35 cm high. The arena was placed in a brown box to reduce visual cues. Mice were placed in the arena and allowed to explore for 5 min, and measured for distance and time travelled and mean speed.

Morris water maze test. The maze was filled with 22–23 °C water that was made opaque with Crayola non-toxic paint, and was located in the centre of a small square room with numerous extra-maze cues (various black shapes on white background, a cabinet and an experimenter). The diameter of the maze was 90 cm and divided into four quadrants (northwest, northeast, southwest and southeast). A circular platform with a diameter of 10 cm was placed 25 cm from the wall in the centre of the northwest quadrant. Visual platform test: the visual platform test was performed on a single day. There were six trials with 30-min inter-trial intervals. In the test, a visible flag was placed on the top of the platform to increase the visibility, and the platform was placed on a random location for each trial. A mouse was placed on water, at the same starting location for all trials, and was measured for latency, distance and mean speed travelled to the platform. Hidden-platform training: mice were first required to swim to and sit on a circular visible platform at 0.5 cm above water level for 10 s. If mice could not find the platform within 60 s, they were gently guided to the platform using a glass stirring rod. Mice were then subjected to five consecutive days of training, consisting of two trials per entry location (entry locations were north, south, east and west) for a total of eight trials per day. The platform was made invisible by submerging it 1 cm below the surface of the water. Mice were expected to find the location of the invisible platform, and measured for latency to reach the platform, distance travelled to reach the platform, path efficiency, time spent in and distance travelled in each quadrant as well as total distance and mean swim speed. Probe trial: on day 6, mice were subjected to a single probe trial, in which the platform was removed and mice were allowed to swim for 60 s. Mice were measured for the amount of time spent in all quadrants, distance and number of times that mice crossed the location of the former platform, and total distance and mean swim speed.

T-maze. Mice were tested for reward (1:1 water/full-fat sweetened condensed milk) (Nestle) on a forced-choice alternation test in a T-maze with an opaque floor and plastic sides. Mice first received food restriction to reduce body weight by 5–10%, and then a 4-day adaptation to the apparatus with the reward. After that, mice were given six pairs of training per day for 12 days, and tests of every 2 days were designated as a trial block. On the first trial of each pair, a mouse was placed in the start arm, forced to choose one of two goal arms in the T (the other is blocked by a removable door), and received the reward at the end. The mouse was kept in this goal arm for 15–20 s and subsequently returned by the experimenter to the start arm. The animal was then given a free choice between two goal arms, rewarded for choosing the 'novel' arm (the one that was not chosen in the first trial of the pair), but punished for choosing the other goal arm (the one that was chosen on the first trial of the pair) using a 20 s-blocking without the reward. The location of the sample arm (left or right) was varied across trials so that mice received equal numbers of left and right presentations, and no more than two consecutive trials with the same sample location. Mice were tested in squads of 4–5 to minimize variations in inter-trial intervals, which was 5–10 min for all animals throughout 12-day training period.

Collagen cross-linking. The method of tail tendon breaking test was used to examine collagen cross-linking, as described[41]. In brief, a collagen fibre was teased from a mid-tail section of the lateral tail tendon and tied to a 2-g weight. The fibre was suspended into a bath containing 7 M urea at 45 °C. The fibre breaking time was determined in quadruplicate for each mouse.

Tissue histology. Skeletal muscles (quadriceps) and dorsal skin were dissected from mice, fixed in 10% neutralized formalin at 4 °C overnight, and embedded into paraffin. Paraffin sections were prepared at 5-μm thickness and subjected to haematoxylin and eosin staining. Images were collected using an Axioskop II light microscope (Zeiss) and analysed using Image J.

Bone volume fraction measurement. We adopted the bone volume fraction procedure established in the literature[42]. In brief, the left intact femurs were removed and analysed via LaTheta LCT-100A X-ray microtomography scanner (Aloka) through mouse physiology core facility at Albert Einstein College of Medicine. The distal part of femur encompassing the cancellous bone was analysed. The trabecular and cortical bone regions were outlined for each tomography slice by the software of the scan system. Bone volume fraction was calculated as the trabecular bone volume divided by the total bone volume. A calibration phantom was used for calibration of each scan.

Immunostaining, histology and western blot. Mice under anaesthesia were perfused with 4% paraformaldehyde, and brains were removed, post-fixed in 4% paraformaldehyde, and infiltrated in 20–30% sucrose. Brain sections were made at 20-μm thickness via a cryostat, blocked with serum, penetrated with Triton-X 100, treated overnight at 4 °C with primary antibody, followed by reaction with fluorescence-conjugated secondary antibody (Jackson), and imaged under a confocal microscope. For BrdU staining, sections were pre-treated with 1 M HCl for 30 min at 37 °C, followed by 5-min treatment with 0.1 M sodium borate, pH 8.5. Primary antibodies included rabbit anti-Iba-1 (Wako), rabbit anti-GFAP (Millipore), mouse anti-TNF-α (Abcam), mouse anti-NeuN (Millipore), and goat anti-Cre antibody (Santa Cruz). For Nissl staining, freshly isolated mice brains were fixed in 4% paraformaldehyde in PBS for overnight at 4 °C. The fixed whole brains were then subjected to cryosectioning coronally, and frozen sections were stained to detect Nissl body by using the NovaUltra Nissl stain kit (IHCWORLD) according to the manufacturer's instruction.

Serial brain sections across the MBH were made at 20 μm thickness, and every five sections were represented by one section with staining and cell counting. For western blotting, animal tissues were homogenized, and proteins were dissolved in a lysis buffer, and western blots were conducted as previously described[3]. Proteins separated by SDS–PAGE were identified by immunoblotting with primary rabbit anti-pRelA, anti-RelA and anti-β-actin antibodies (Cell Signaling) and horseradish peroxidase (HRP)-conjugated anti-rabbit secondary antibody (Pierce).

DNA vectors, cell culture and molecular/biochemical analysis. Promoter sequence of the rat *Gnrh1* gene was PCR amplified (−1934 to +21) from a rat genomic DNA preparation, and subcloned into the pGL3-basic luciferase reporter vector (Promega) using standard cloning strategies. pcDNA expressing ^{CA}IKK-β or ^{DN}IκB-α versus control were previously described[13–15,37], or pcDNA expressing HA-RelA was provided by A. Lin. RelA shRNA and control (GFP) shRNA vectors were obtained from Addgene, as studied in the literature[43]. RelA shRNA: 5′-GCATGCGATTCC GCTATAA-3′; control shRNA: 5′-ACAGCCACAACGTCTATAT-3′. Expression plasmids for c-Jun or c-Fos were provided by D. Stocco. Vectors expressing c-Jun or c-Fos shRNA or scramble shRNA control were provided by L. Fahana. c-Jun shRNA: 5′-AGTCATGAACCACGTTAAC-3′; c-Fos shRNA: 5′-TCCGAAGAG AACGGAATAA-3′; scramble shRNA: 5′-GTTATTACTGTTCGATCGC-3′. 12-*O*-tetradecanoylphorbol-13-acetate (also known as phorbol 12-myristate 13-acetate or TPA) and calphostin-C were from Sigma-Aldrich. TPA or calphostin-C was

dissolved in dimethylsulphoxide (DMSO) and applied in cell culture medium at a final concentration of 0.2 μM or 0.01 μM, respectively, and DMSO did not exceed 0.1% of cell culture medium. GT1-7 cells were previously described[13], and cultured in a standard humidified incubator at 37 °C and 5% CO_2 with DMEM cell culture medium supplemented with 10% FBS, 2 mM L-glutamine, and PenStrep (50 U ml^{-1} penicillin G, 50 μg ml^{-1} streptomycin). Transfection of cultured cells with luciferase plasmids and expression plasmids was performed through Lipofectamine 2000 (Invitrogen). The dual luciferase reporter assay (Promega) was performed according to the manufacturer's instruction, and co-transfection of the pRL-TK vector expressing *Renilla* luciferase was used to control firefly activity internally. Empty plasmids pGL3 and pcDNA3.1 were used as negative controls. RNA was extracted by TRIzol (Invitrogen) and analysed via SYBR green real-time PCR (StepOnePlus real-time PCR system, Invitrogen). Testosterone and oestradiol were measured using testosterone and oestradiol EIA kits (Cayman Chemical). GnRH was measured using the luteinizing hormone-releasing hormone EIA kit (Phoenix Pharmaceuticals).

BrdU labelling study. Mice were pre-implanted with intracerebroventricular (i.c.v.) cannula in the hypothalamic third ventricle, and after a ~3-week recovery, they were subjected to neurogenesis assay or survival assays. In the neurogenesis assay, mice were daily pre-injected with GnRH or vehicle at the dose of 1 ng per day through cannula for 3 days, subsequently a single i.c.v. injection of BrdU (Sigma) at the dose of 10 μg (defined as day 0), and continued to receive daily i.c.v. injections of GnRH (1 ng per day) or vehicle for 7 days before they were killed for brain sectioning. In the survival assay, mice pre-received daily i.c.v. injections of GnRH (1 ng per day) or vehicle for 3 days, then daily i.c.v. injections of BrdU (10 μg per day) together with daily i.c.v. injections of GnRH (1 ng per day) or vehicle for 7 days (last day was defined as day 7), and followed by continued daily i.c.v. injections of GnRH (1 ng per day) or vehicle until day 30 when mice were killed for brain sectioning.

Statistical analyses. Kolmogorov–Smirnov test was used to determine parametric distribution of data. Analysis of variance (ANOVA) and appropriate post-hoc analyses were used for comparisons involving more than two groups. Two-tailed Student's *t*-tests were used for comparisons involving only two groups. Lifespan analysis was performed using Kaplan–Meier survival analysis; the mutant and control survivorship curves were compared in pairs and *P* values were obtained with log-rank test. Maximal lifespan of mice were statistically analysed using Chi-squared test according to the literature[44]. All data were presented as mean ± s.e.m. $P < 0.05$ was considered significant.

37. Meng, Q. & Cai, D. Defective hypothalamic autophagy directs the central pathogenesis of obesity via the IκB kinase β (IKKβ)/NF-κB pathway. *J. Biol. Chem.* **286,** 32324–32332 (2011).
38. Banks, W. A. *et al.* Effects of a growth hormone-releasing hormone antagonist on telomerase activity, oxidative stress, longevity, and aging in mice. *Proc. Natl Acad. Sci. USA* **107,** 22272–22277 (2010).
39. Tillerson, J. L. & Miller, G. W. Grid performance test to measure behavioral impairment in the MPTP-treated-mouse model of parkinsonism. *J. Neurosci. Methods* **123,** 189–200 (2003).
40. Mueller, J. M. & Pahl, H. L. Assaying NF-κB and AP-1 DNA-binding and transcriptional activity. *Methods Mol. Biol.* **99,** 205–216 (2000).
41. Flurkey, K., Papaconstantinou, J., Miller, R. A. & Harrison, D. E. Lifespan extension and delayed immune and collagen aging in mutant mice with defects in growth hormone production. *Proc. Natl Acad. Sci. USA* **98,** 6736–6741 (2001).
42. Ramanadham, S. *et al.* Age-related changes in bone morphology are accelerated in group VIA phospholipase A2 (iPLA2β)-null mice. *Am. J. Pathol.* **172,** 868–881 (2008).
43. Meylan, E. *et al.* Requirement for NF-κB signalling in a mouse model of lung adenocarcinoma. *Nature* **462,** 104–107 (2009).
44. Wang, C., Li, Q., Redden, D. T., Weindruch, R. & Allison, D. B. Statistical methods for testing effects on "maximum lifespan". *Mech. Ageing Dev.* **125,** 629–632 (2004).